

Convenient and Efficient Elimination of Heavy Metals from Wastewater Using Smart Pouch with Biomaterial

Malik, R.¹ Saini, N.¹ Ahlawat, S.² Singhal, S.³ and Lata, S.^{1*}

1. Department of Chemistry, Deenbandhu Chhotu Ram University of Science and Technology, P.O.Box-131039, Murthal, Haryana, India
2. Department of Chemistry, Maharshi Dayanand University, P.O.Box-124001, Rohtak, Haryana, India,
3. Department of Chemistry, Deshbandhu College, University of Delhi, P.O.Box-110019, Delhi, India,

Received: 11.03.2018

Accepted: 20.06.2018

ABSTRACT: A newly developed Smart Pouch with enclosed biomaterial (*Aloe vera* and coconut husk powder) has been experimented for elimination of heavy metals i.e. (Pb^{2+} , Cu^{2+} , Ni^{2+} and Zn^{2+}) from wastewater. The effect of concentration, pH, temperature, contact duration etc. was investigated using batch experiments which resulted that the Pouch may be accepted for convenient, efficient and low-cost accumulation of several heavy metals simultaneously from waste water. The maximum Pb removal was 99.99%, 93.21% for Cu, and for Ni, it was 91.97% whereas for Zn, 86.41% was obtained and also, the uptake capacity of pouch was quite sensitive towards initial metal concentration in the studied range of 10-200mg/L present in wastewater. The findings were further interpreted by quantum chemical study as theoretical support, various adsorption isotherms, FTIR, SEM, XRD, and physiochemical properties of metal ions to justify the synergized performance of new Pouch. A good correlation was found between experimental methods and theoretical findings.

Keywords: Accumulation, *Aloe vera*, Coconut husk, Quantum study.

INTRODUCTION

The continuous growth of environmental pollutants due to accelerated industrial development and increasing needs of human being have led to the serious concern among present day scientists. Although, the concept of clean and green environment involves the deep insight into each type of pollution (air, water and soil) management, though the wastewater management has attracted the present day researchers quite a lot and the search for soft and effective technologies has been adopted to remove the pollutants (He et

al., 2011) Although the use of several plant products has been exercised during the past decade in order to accumulate quite a large amount of heavy metals through adsorption phenomenon (Pellera et al., 2012)but the study of their synergized influence is not much explored till date. Also, the bio-sorption is the modest process where low-cost dead biomass is being utilized for the sequestering of heavy metals (Reddy et al., 2005) This process has been found as a low cost and highly efficient pollution removal method and minimizes the quantity of the chemical as well as biological sludge to be

* Corresponding Author, Email: sumanjakhar.chem@dcrustm.org

disposed off. During application of bio-sorption method, microorganisms are preserved and no maintenance and nutrition is further required (Reddy et al., 2005) Biodegradable starch-based polymers have been studied which inferred that these materials possess quite good characteristics and hence, found to be suitable for use in heavy metal removal from waste water. It is convenient to use natural polymers due to their abundance, biocompatibility and biodegradability in the nature. Polymeric blends may also be prepared for removal of heavy metals with the help of natural polymers (biosorbents). Interestingly, new materials based on blends of two or more polymers have been noticed now a days. Blends and mixtures of synthetic and natural polymers or those of two or more natural polymers can create a new class of materials with enhanced mechanical properties and biocompatibility as compared with those of the single components (Okafor, 2012 ; Giusti et al., 1994).).Several natural polymers can be blended with another naturally occurring polymer to develop new and modified materials by means of physical blending. Physical blending may be considered as the simple mixing of polymeric materials in their melt state or in any solvent like xylene, toluene etc in finely divided form, with no occurrence of chemical reactions (Arcana et al., 2007). It is an easier route to prepare new materials with the required combination of properties. The modification of polymers using blending technique is a mature technology which was developed in the 1970s or may be even earlier. (Arcana et al., 2007 ; Miles et al., 2004)Moreover, blending can also be carried out by using conventional machinery without any expensive investment e.g. industry using ball mills (Abdeen et al., 2015). In order to meet the requirements of the targeted application, this approach can be exploited due to its wide range of properties in short time as well as for low cost (Wang et al., 2011; Slatter et al., 2003]. Blending may improve the properties to a certain

application, or even maximize the performance of a material (Scott, 2000; Chiellini, 2006).

Though, the recent researchers in the present field are exploring different kind of nanoparticles as adsorbents for heavy metals and other pollutants elimination (Kaushal et al., 2017; Arief et al., 2008; Bueno et al., 2008; Shen et al., 2004) from aqueous media, specially, nanomagnetic particles (Kaushal et al., 2017), where the risk of iron exists, being another heavy metal, may get injected in higher doses than permitted level, in the cleaned water through these processes which make use of nanomagnetic particles. So, the use of biomaterial, being safer, low-cost, conveniently available will always persist as the centre of attraction for the modern age scientists for this problem.

The negligible exploration of combined/synergistic study of two polymers/biodegradable plant materials being used for elimination of heavy metals, herein, motivated the authors for the present study which describes about simultaneous accumulation of heavy metals (Pb^{2+} , Cu^{2+} , Ni^{2+} and Zn^{2+}) from wastewater through adsorption characteristics. An empty Tetley tea Pouch filled with the biomaterial (PB) prepared from *Aloe vera* (L.) Burm.f. and Coconut husk fine powders has been evaluated in the study. The theoretical approach has also been exercised to extract the support from quantum study of the major component of *Aloe vera* as well as that of coconut husk (*Cocos nucifera* L.) and the obtained information has further been implemented to suggest a suitable mechanism for adsorption.

Material & Methods

Aloe vera as well as coconut husk were collected from Sonipat, Haryana, India in order to study as biomaterial with a fresh approach. *Aloe vera* (Synonym: *Aloe barbedensis*) complete leaf cut to small pieces(1cm x 1cm) was shed dried about one month, then dried in oven at 60°C for

24h and Coconut Husk (*Cocos nucifera* L.) collected almost in dry condition, further dried in the oven at 60°C for an hour. Thereafter, both the biomaterials were ground separately in fine powder with mechanical grinder, then sieved through 100nm pore size. To prepare new biomaterial, these two powders(0.5g each) were blended (1:1w/w) in 100mL xylene supplied by Qualigens fine chemicals, Mumbai, India with minimum assay 99% at 110°C. The mixture was stirred for 4 hours at 600rpm then, xylene was evaporated and the new biomaterial was dried under vacuum at room temperature (Arcana et al., 2007). Thereafter, the observed immiscible biomaterial was preserved under vacuum till further use.

The observed immiscible biomaterial containing *Aloe vera* and coconut husk powders in blended form was filled in weighed empty Tetley tea Pouch, India, and this Pouch containing new biomaterial i.e. Smart Pouch named as Pouch with Biomaterial (PB) was further used for adsorption purposes in all the batch experiments in order to eliminate the four metals present in wastewater.

All the chemicals used in the experiments were of analytical grade and they were used without further purification. All the solutions were made in de-ionized water. Different solutions of heavy metals (Cu(II), Pb(II), Ni(II) and Zn(II)) supplied by Qualigens fine chemicals, Mumbai, India (minimum assay 99%) were prepared from the solution containing 200 mg/L as stock solution as well as one of the test solution and further dilutions were made as 150 mg/L, 100 mg/L, 75 mg/L, 50 mg/L and 10 mg/L. The pH of the aqueous

solution was 5.0, which did not change much with dilution. For experiments at different pH, the acidity of heavy metal (Cu(II), Pb(II), Ni(II) and Zn(II)) solutions were adjusted by addition of 0.1M HNO₃ and 0.1M NaOH solution drops.

The experiments for metal removal were carried out in conical flasks by agitating a pre-weighed amount of the biomaterial powder which was then, trapped in the empty tea Pouch (with 0.15g average weight), known as Smart Pouch(PB) with 100mL of the aqueous heavy metal solution in a constant temperature water bath shaker (NSW, Mumbai) for a pre-determined time interval at a constant speed of 200rpm. After this, the mixture was filtered and remaining heavy metal in solution was determined with atomic absorption spectrometry (Labindia Analytical AA-7000). The amount of heavy metal adsorbed per unit mass of the biomaterial was computed by using the eq-1.

$$q = \frac{C_0 - C_e}{M} \quad (1)$$

where C_0 and C_e are heavy metal concentrations in mg/L before and after adsorption for time in min., and M is the amount of adsorbent in g taken for 1 L of heavy metal solution. The extent of adsorption in percentage is found from the eq-2.

$$Adsorption\% = \frac{C_0 - C_e}{C_0} \times 100 \quad (2)$$

All the batch studies were performed in triplicate within error ratio of $\pm 0.5\%$. To investigate the effect of various operational parameters like pH, temperature etc., the following experimental conditions were opted for different batch experiments (Table-1).

Table 1. Experimental conditions for batch experiments

Amount of biomaterial (g)	0.2, 0.4, 0.6, 0.8, 1.0, 1.2
Initial Metal Concentration (mg/L)	10, 50, 75, 100, 150 and 200
pH (Initially)	2.0, 3.0, 4.0, 5.0, 6.0, 7.0 and 8.0
Agitation time (min.)	10, 20, 30, 40, 50, 60, 70, 80, 90, 100, 110 and 120
Adsorption temperature (°C)	10, 20, 30, 40, 50, 60, 70 and 80
Particle size (µm)	100 only

The quantum chemical studies were performed for the present biosorbent using AM1 (Austin Model1), a semi empirical method based on the neglect of differential diatomic overlap approximation. The quantum parameters were calculated using HyperChem Professional 8.0 package (Hypercube Inc., USA). The following quantum chemical descriptors were taken into consideration: energy of the highest occupied molecular orbital (E_{HOMO}), energy of the lowest unoccupied molecular orbital (E_{LUMO}), energy gap: $\Delta E_{\text{gap}} = E_{\text{LUMO}} - E_{\text{HOMO}}$ and dipole moment (μ) of major constituent of both the biopolymers. The technique was studied to correlate the various quantum descriptors with the observed experimental data and hence, a novel mechanism of adsorption of metals has been suggested.

Surface morphology of new blend before and after adsorption was imaged under Model Zeiss Ultra 55 at 3kV for SEM technique at x1000 magnification.

The FTIR of fine powder of the studied new biomaterial before and after adsorption was recorded by Perkin-Elmer FT-IR/RZX. The spectrum ranges from 4000 cm^{-1} - 400 cm^{-1} .

RESULTS & DISCUSSION

Fourier transform infrared (FTIR) spectroscopy has been applied to investigate

specific molecular interactions in biomaterial Pouch. When two polymers (*Aloe vera* and coconut husk powder) after blending are immiscible i.e. in separate and distinct phases and it may be considered in IR spectral terms that the two components do not react chemically (Arief et al., 2008). In this case, the FTIR spectrum of the blend reflects the peaks addition of the IR spectra of the two individual components. In the case of miscible or partially miscible polymers, the IR spectra may arise differently due to the formation of new bands as a result of their miscibility as well as the disappearance of some earlier noticed peaks (Arief et al., 2008). Moreover, the presence of the functional groups are evidenced by the FTIR peaks as given in Fig.1. The peak of phenolic -OH was observed with less considerable shift after adsorption whereas -C-O-C- stretching before and after adsorption gives a major shift but towards higher wave number after adsorption (1060 cm^{-1} before adsorption shifted to 1099 cm^{-1} after adsorption). This behavior may be observed due to binding of HM (heavy metal) ions to the various electron rich centers (oxygen) and the increase in wave number for -C-O-C- stretching may originate due to trapping of HM ions in between the two polymers interface.

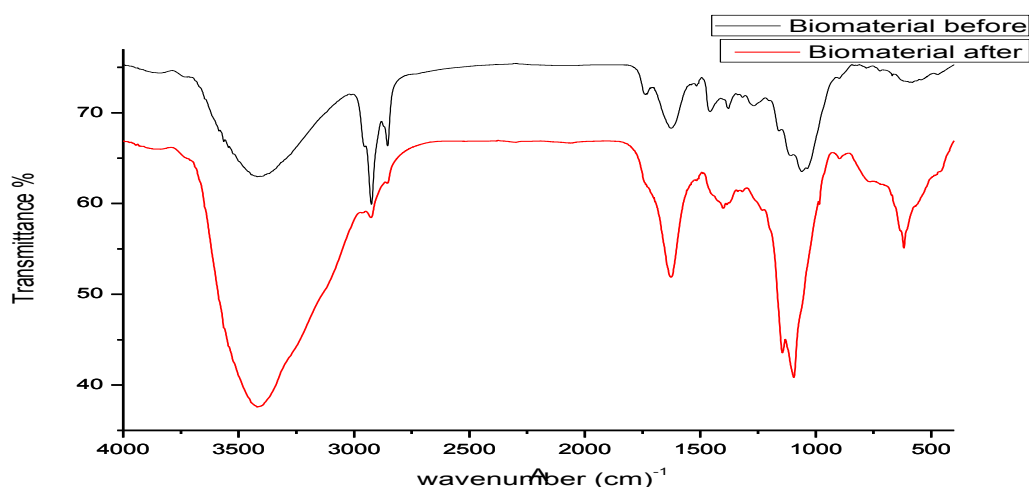


Fig. 1. FTIR of new biomaterial before and after adsorption

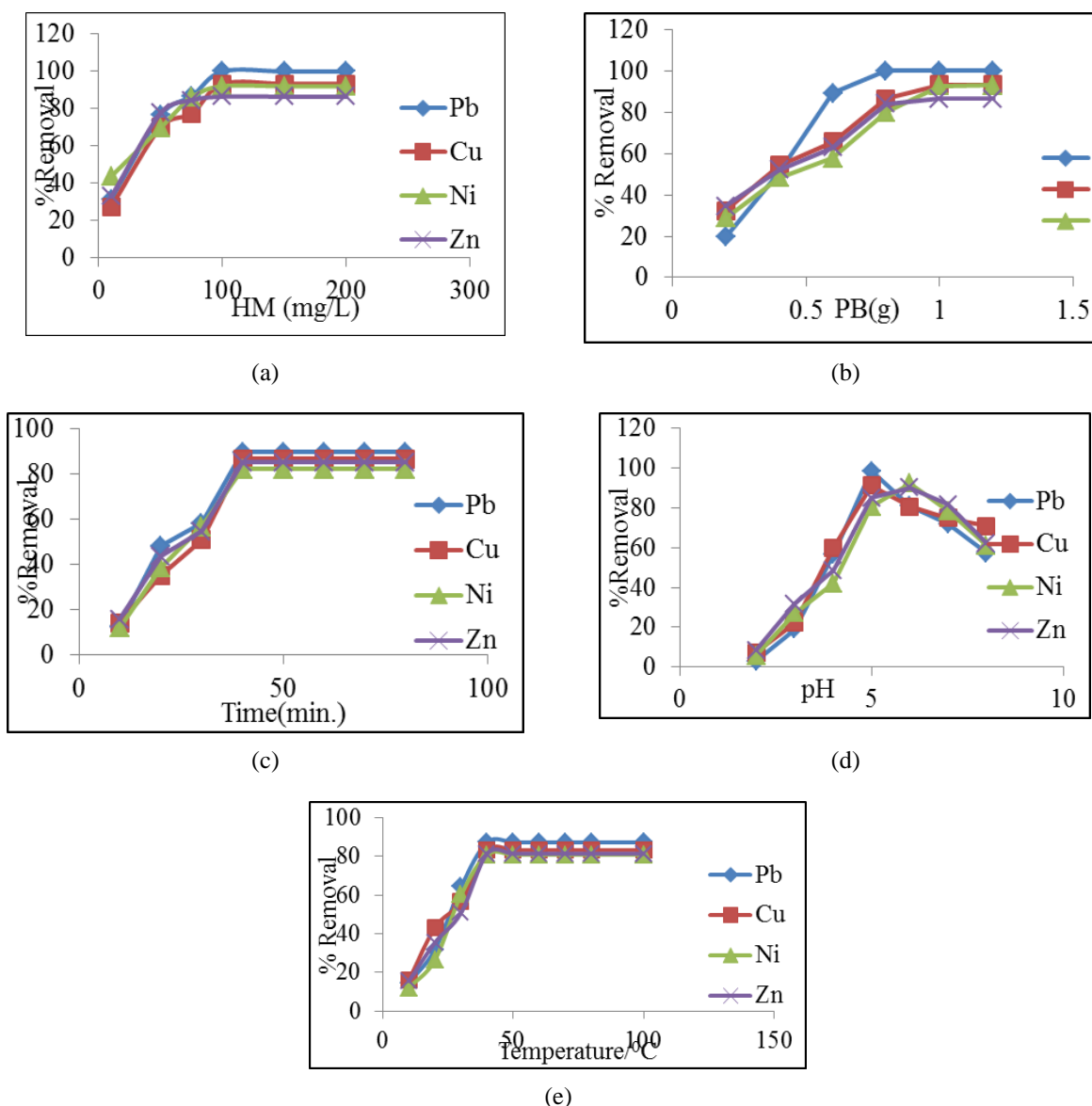


Fig. 2 (a) Variation of initial metal ion concentration, (b) Different biomaterial doses (c) Effect of contact time, (d) Effect of pH and (e) Effect of temperature on adsorption of heavy metals 100mg/L each [(Pb(II),Co(II),Ni(II),Zn(II)], Biomaterial- 1.0 g, pH-6.0, with contact time (40min) and Orbital shaking speed=200rpm at 30±1°C

The optimization regarding determination of the best doses of HM ions for adsorption of Cu(II), Pb(II), Ni(II), and Zn(II) ions was accomplished with six different (10-200 mg/L shown in Table 1) initial metal ions concentration. The adsorption results are plotted in Fig. 2(a). It is generally found that the removal is low at lower concentration (10 mg/L). At low metal concentration, there is not enough availability of ions to be uptaken by the biomaterial. For low doses, the binding

sites are occupied by metals ions quickly and as a result there is no further uptake. Among the six initial HM concentrations, 100 mg/L showed highest removal i.e. 99.99% for Pb(II), 93.21% for Cu(II), 91.97% for Ni(II) and 86.41% for Zn(II) ions and afterwards optimization was reached. It was also noticed that in this Figure, zigzag curves crossing each other during elimination process for all the four metals are obtained. This discrepancy of adsorption behavior may be described due

to availability of different nature of PB active sites for adsorption during whole concentration range for each HM ion (metal speciation) and consequently, in case of Pb, not a separate curve without cross over among four metals Fig.2(a) is obtained and which may be thought due to the immiscible nature of Pouch material (Bueno et al., 2008; Shen et al., 2004).

All the batch experiments were carried out under the experimental conditions as mentioned in Table1 and optimization for the best doses of HM ion concentration for obtaining maximized adsorption of Cu(II), Pb(II), Ni(II), and Zn(II) ions, batches were accomplished with (0.2, 0.4, 0.6, 0.8, 1.0 and 1.2g) biosorbent doses. The observed results are plotted in Fig. 2(b) which shows that at lower doses of adsorbent, % removal is low but gets acceleration with increase of biomaterial dose and reaches at highest (optimization level) around 1.0g of the biomaterial filled in the Smart Pouch due to equilibration since, mostly, all the available active sites are occupied by HM ion (Shen et al., 2004). The cause of increased % removal may be understood due to more and more availability of active sites with the higher doses of biosorbent. Regarding this Pouch, the order of % removal is Pb>Cu>Ni> Zn particularly at higher biomaterial dose.

The effect of contact time on removal of Cu(II), Pb(II), Ni(II) and Zn(II) was investigated with initial concentration of each HM but all at one time i.e. 100 mg/L with an optimized dose of 1.0g biomaterial filled in the Pouch (PB) at $30\pm 1^\circ\text{C}$. The adsorption experiments were observed using batch process under the earlier described experimental conditions Fig. 2(c). During initial exposures of HM ions towards biomaterial sites, nearly up to first 40 min., there is strong competition for adsorption among all the metals showing faster rates of removal for Zn and slower removal rates for Cu before their optimized contact time (~40 min) with precise order

of % removal obtained as Pb>Cu>Zn>Ni. There was quite large numbers of vacant active sites readily available for binding during the first phase of the experiment and large amount of metal ions got bound rapidly on PB at the first go of adsorption. After that, these binding sites become limited in number, and still some vacant surface sites if available, become difficult to be occupied simultaneously by Cu(II), Pb(II), Ni(II) and Zn(II) ions due to the formation of repulsive forces between the metals ions on the solid surface and the liquid phase. Hence, due to near saturation level for the sites, the driving force of mass transfer between liquid and solid phase in an aqueous adsorption system decreases with time phase. Further, the metal ions have to pass through the deeper surface of the pores due to the presence of lignin and hemicellulose as water insoluble matter in PB (Grimwood et al., 1975) for binding and face a confronting situation with much larger resistance which results in the slowing down of the adsorption during the later time phase (Pagnanelli et al., 2003; Romera & Romera 2007)

The effect of pH on the elimination of Cu(II), Pb(II), Ni(II) and Zn(II) ions by Pouch were conducted between pH 2.0 and 8.0 and are shown in Fig. 2(d). Generally, the adsorption capacities of Pouch filled with biomaterial for removing Cu(II), Pb(II), Ni(II) and Zn(II) ions were strongly affected by the pH value, which reflects that with increase in the solution pH , increase in adsorbed amount of HM ions and each HM ion shows optimization behavior at different pH levels, after which, the % removal shows a sharp decrease because precipitation of HM ion as its hydroxide gets initiated. Many adsorption studies have reported that pH (5.0 - 7.0) as the optimized pH value for Cu(II), Pb(II),Ni(II) and Zn(II) adsorption by using different biosorbents (Das et al., 2007; Fiol et al., 2006). As the number of H^+ ions is quite high at low pH (2.0 - 3.0)

to compete with Cu(II), Pb(II), Ni(II) and Zn(II) ions for the available adsorption sites of the new Pouch. Additionally, most of the functional groups present in the PB get protonated at low pH value (Das et al., 2007; Fiol et al., 2006). thereby, decrease in the number of binding sites available for the adsorption of metal ions. The enhanced adsorption capacity at higher pH values may lead to the lowered number of H⁺ ions (Das et al., 2007) In case of Pb, Cu and Ni showed maximum % removal at pH-5.0 and Zn at 6.0 pH. The gradual decrease in the uptake of metal by PB may be explored on the basis of:

With the increase of pH, specifically after pH-7, the precipitation in the form of metal hydroxide [HM(OH)₂] where HM=Cu²⁺, Pb²⁺, Ni²⁺ and Zn²⁺ may occur (Sadeek et al., 2015). Afterwards, diffusion of these slightly soluble species (Sadeek et al., 2015) in aqueous medium (metal hydroxides) in the pH range 7-8, with higher number of OH⁻ ions as well as the biosorbent which also contains OH⁻ centres and other electron rich centres, hence chances of repulsion among OH⁻ ions coming from both locations (solution and biosorbent) and other negative centres present on PB may resist the capacity of metal ions to approach the available sites on PB for adsorption at higher pH.

Another point of consideration may be stated that in the range of 7-8 pH, complete precipitation may not be established and only partial precipitation happens due to which the complete removal of metal ions as their hydroxides may not accomplish.

The adsorption of the metal ions on the Pouch containing new biomaterial was investigated at different temperatures using water bath with temperature control and results are notified in Fig.2(e). For kinetic studies, biosorption was carried out using 100mL of each batch experiment but all metals simultaneously. A general trend is observed for all the HM ions which shows

enhancement of % removal, but to different extent for each metal ion with increasing temperatures. The decreased % removal may be due to the initiation of desorption process after optimization (around 70^o-80^oC) (Fiol et al., 2006). In case of Pouch, initially, at lower temperatures (10^oC to 45^oC), again the varying and confronting situation with strong tendency for getting adsorbed for each metal crossing each other Fig.2(e), may be due to the availability of different kind of adsorption sites present in the Pouch of coconut husk and *Aloe vera* leaf powder and the reaction kinetics and optimization level may be due to blending process.

Gibbs free energy (ΔG), enthalpy of adsorption (ΔH), and entropy of adsorption (ΔS) data was computed and hence, the thermodynamic criteria for the adsorption were evaluated by carrying out the adsorption experiments by varying temperatures and using eq-3 and 4.

$$\Delta G = \Delta H - T\Delta S \quad (3)$$

$$\log \left[\frac{q}{c_e} \right] = -\frac{\Delta H}{2.303RT} + \frac{\Delta S}{2.303R} \quad (4)$$

where (q/C_e) is the adsorption affinity i.e. the ratio of amount adsorbed per unit mass at equilibrium (q) to the equilibrium concentration of the adsorbate (C_e). Further, ΔH and ΔS were obtained from the slope and the intercept of the Van't Hoff plots of $\log (q/C_e)$ versus $1/T$ (eq-4) whereas, ΔG values using eq-3. The negative values of ΔG assure that the adsorption process is spontaneous and data presented in Table 2 explains the fact that the adsorption process becomes gradually more spontaneous towards elevated temperatures (Sun et al, 2008; Freundlich, 1906). The ΔH values indicate that the process could be endothermic in nature but the positive sign of entropy change suggests considerable fraction of water molecules got removed from the hydration shell of metals (Ali et al, 2015)

Table 2. Thermodynamic parameters for adsorption of heavy metal ions on new biomaterial (1.0g) concentration at different temperatures (pH=6.0).

Heavy Metals	ΔS Jmol ⁻¹	ΔH kJmol ⁻¹	ΔG (kJ/mol) at temperature		
			30°C	60°C	80°C
Cu	23.74	0.41	-6.77	-7.48	-7.96
Pb	20.29	0.38	-5.76	-6.37	-6.77
Ni	18.03	0.36	-5.10	-5.64	-6.00
Zn	19.48	0.35	-5.54	-6.13	-6.52

Langmuir adsorption isotherm supports in analyzing the equilibrium data in accordance with the eq-5.

$$\frac{C_e}{q} = \frac{1}{q_{max}} K_d + \frac{C_e}{q_{max}} \quad (5)$$

where K_d is the Langmuir constant i.e. energy of adsorption (L/mg). If the Langmuir equation is obeyed by the adsorption equilibrium, so, plot of (C_e/q) vs. C_e should supply a straight line (Fig.7), the slope and intercept of which are exploited to calculate q_{max} and K_d respectively and K_d values also satisfy the observed order of metal removal (Ali et al., 2015; Langmuir, 1916). The R^2 means the regression coefficient values of different isotherms placed in Table 3 show that this model fits very well. Thermodynamic data for adsorption of metal ions on PB surface at different concentrations and at 30°C–80°C with pH- 5.0 is shown in Table 3.

Freundlich isotherm model, quite important for heterogeneous adsorption systems with uniform energy (eq-6).

$$q = K_f C_e^{1/n} \quad (6)$$

where K_f and n are known as Freundlich coefficients and both constants can be obtained from the plots of $\log q$ versus $\log C_e$ on the basis of the linear form of the eq-7.

$$\log q = \log K_f + \frac{1}{n} \log C_e \quad (7)$$

The slopes ($1/n$) of the plots (0.14 for Pb²⁺) are found to be in the range of 0 to 1, proving its better intensity of adsorption or surface heterogeneity i.e. slight chemisorption also occurs in addition to physical adsorption, given in Table 3

whereas $1/n$ is 1.88 for Cu, 4.09 in case of Ni ions and 2.55 for Zn may show co-operative adsorption of physical type (Freundlich, 1906; Ali et al., 2015; Rao & Bhole, 2001; Haghseresht & Lu, 1998) as these values exceed 1.

Temkin isotherm (Foo & Hameed, 2010) explicitly considers the adsorbent–adsorbate or adsorbate–adsorbate interactions. The model also assumes that heat of adsorption (function of temperature) of all molecules in the layer would decrease linearly with surface coverage (Foo & Hameed, 2010) and the adsorption is characterized by uniform distribution of binding energies. The Temkin isotherm has the following linear form expressed by eq-8.

$$q = B \ln A_T + B \ln C_e \quad (8)$$

$$B = \frac{RT}{b_T} \quad (9)$$

where, A_T is Temkin isotherm equilibrium binding constant which corresponds the maximum binding energy (L/mg), R is the universal gas constant (8.314 Jmol⁻¹K⁻¹), B is a constant related to the heat of sorption (J/mol), T at 30±1°C, b_T is Temkin isotherm constant, which indicates the adsorption potential of any adsorbent for a specific metal and herein, A_T as well as b_T values exactly favor the observed order of removal i.e. Pb>Cu>Ni>Zn (Table 3). Both A_T and B can be determined from a plot q vs. $\ln C_e$ (Fig. 3c) and these constants were determined from the intercept and slope, respectively.

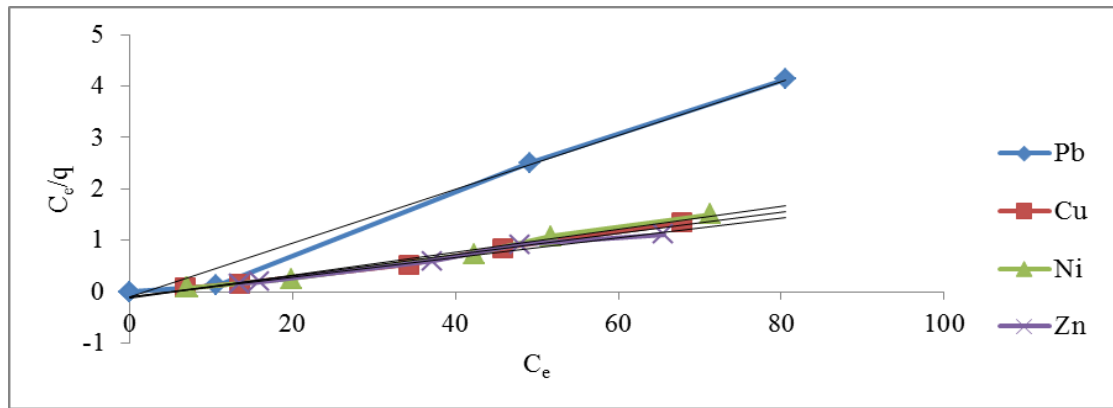


Fig. 3(a) Langmuir plots for adsorption of heavy metals on PB

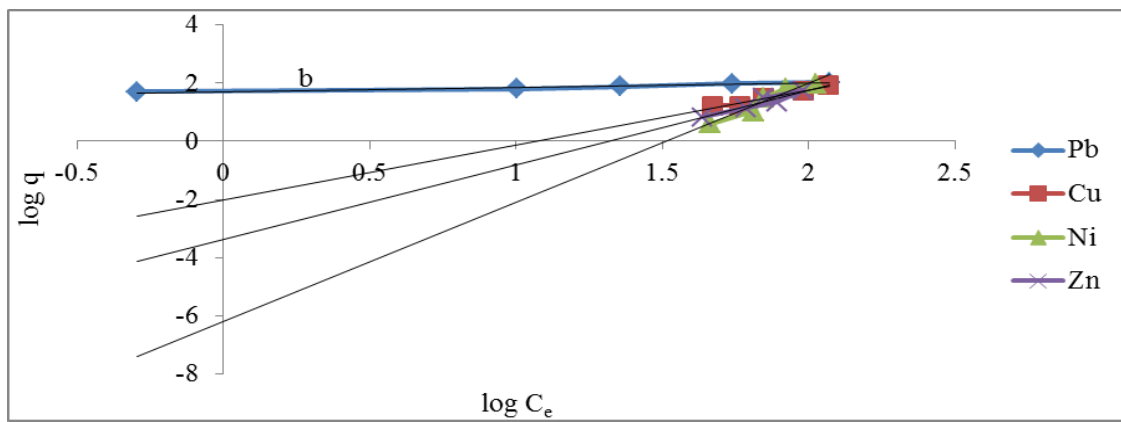


Fig. 3(b) Freundlich plots for adsorption of heavy metals on PB

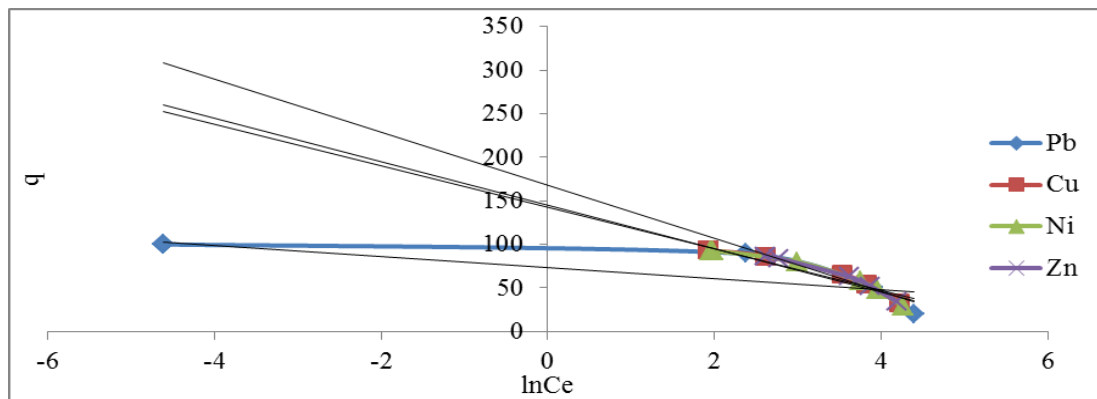


Fig. 3(c) Temkin plots for adsorption of heavy metals on new Pouch

Table 3. Isotherm parameters for PB

Biomaterial 1.0 (g)	Langmuir constants			Freundlich constants			Temkin constants		
	R ²	q _{max} (mg/g)	K _d (L/mg)	R ²	1/n	K _f (L/mg)	R ²	A _T (L/mg)	b _T (J/mol)
Pb	0.9907	19.15	0.550	0.9532	0.14	1.71	0.7101	26.71	398.85
Cu	0.9910	48.30	0.207	0.9604	1.88	1.99	0.9266	13.75	105.62
Ni	0.9889	45.45	0.179	0.9349	4.09	6.19	0.9264	13.40	100.96
Zn	0.9855	52.63	0.187	0.9240	2.55	3.36	0.9685	12.65	82.56

Adsorption may occur through adsorbate diffusion or bulk diffusion, diffusion from the film to the biosorbent surface i.e. film diffusion or external diffusion, intraparticle diffusion or pore diffusion and also adsorption of metals or physico-chemical adsorption or by complexation too, occurring in the sequential steps (Ali et al., 2015; Ho et al., 2000; Prasad & Saxena 2004; Malik et al., 2015; Hameed et al., 2008). In the present case, the rate may not be limited by mass transfer from the bulk liquid to the PB external surface due to proper agitation, so bulk diffusion was minimized. Hence, external diffusion or film diffusion and intraparticle diffusion may occur resulting to the metal adsorption by physico-chemical adsorption and/or partial complexation which might control the overall adsorption process. The dynamics of metal adsorption onto the PB has been obtained by time profile for adsorption of Pb, Cu, Ni and Zn ions using batch contact time studies. For all metals, the sorption was rapid as equilibrium was attained within 40 minutes.

Three models for adsorption kinetics of metals were estimated i.e. pseudo-first-order, pseudo-second-order and intraparticle diffusion models for the present study. The straight-line fits of the pseudo-second-order (t/q_t versus t , eq-10) with (Fig. 4b), intraparticle model, q_t versus $t^{1/2}$ (Fig. 4c) and eq-11, pseudo-first-order [$\log(q - q_t)$ versus t , eq-12 (Fig. 4a)].

$$\frac{1}{q_t} = \frac{1}{k_2 q^2} + \left[\frac{1}{q} \right] t \quad (10)$$

Following the Intraparticle diffusion [30] shown by eq-13:

$$q_t = k_{pi} t^{1/2} \quad (11)$$

where k_{pi} ($\text{mg/g min}^{1/2}$), the slope of the straight line of q_t versus $t^{1/2}$ (Fig. 4c) shows the rate parameter of stage i whereas C_i ,

the intercept of stage i , gives an idea about the thickness of boundary layer. This theory tells that, larger the intercept, the greater the boundary layer effect (Ali et al., 2015; Prasad, 2004).

$$\log(q - q_t) = \log q - k_{pi} \frac{t}{2.303} \quad (12)$$

where q and q_t signify the amount adsorbed at equilibrium and at any time t , k_{pi} is the rate constant. The graph of $\log(q - q_t)$ versus t (Fig. 4a) possesses straight lines at different concentrations. If intraparticle diffusion occurs, then q_t versus $t^{1/2}$ will be linear (Prasad, 2004). possessing slope as well as intercept, then, some kind of phenomenon i.e. instantaneous adsorption or external surface adsorption i.e. first region in Fig. 4(c) along with intraparticle diffusion also may be observed, otherwise plot passes through the origin, and the rate limiting process is controlled solely by the intraparticle diffusion. So, external diffusion or film diffusion and intraparticle diffusion may take place, and consequently, the metal adsorption by partial complexation and/or physico-chemical adsorption (electrostatic forces) might govern the overall process. The various kinetics parameters of three models are shown in Table 4 and the dependence of metal ion concentration on the rate constant $k_{i(1)}$ and $(k_{i(2)})$, all these parameters support in describing the mechanism (Phuong et al., 2010) and the variation in the rate should be proportional to the first power of the concentration if only surface adsorption occurs strictly. In the current study, pseudo-first-order kinetics is followed satisfactorily with high R^2 values greater than 0.99 except Zn which is 0.98 along with slight intraparticle diffusion too, whereas pseudo-second-order is not followed at all. Moreover, the C_i values placed in Table 4 verify the observed order of metal removal.

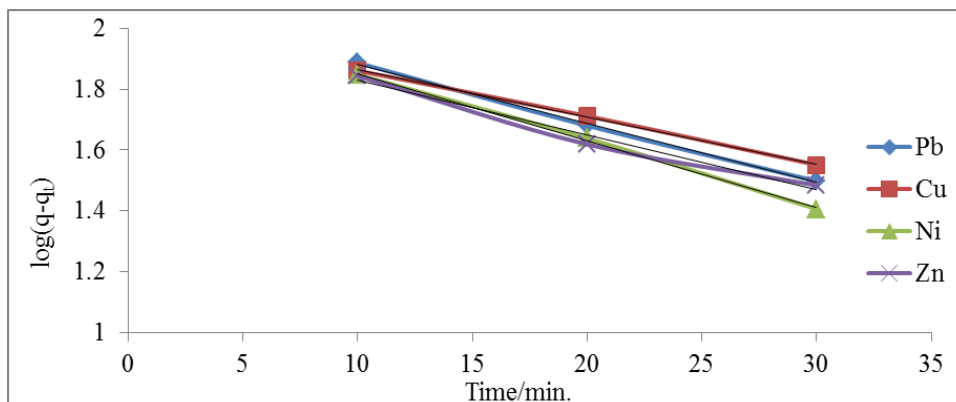


Fig. 4(a) Pseudo-First-order kinetics (plot of time vs. $\log(q - q_t)$) for heavy metal biosorption on PB.

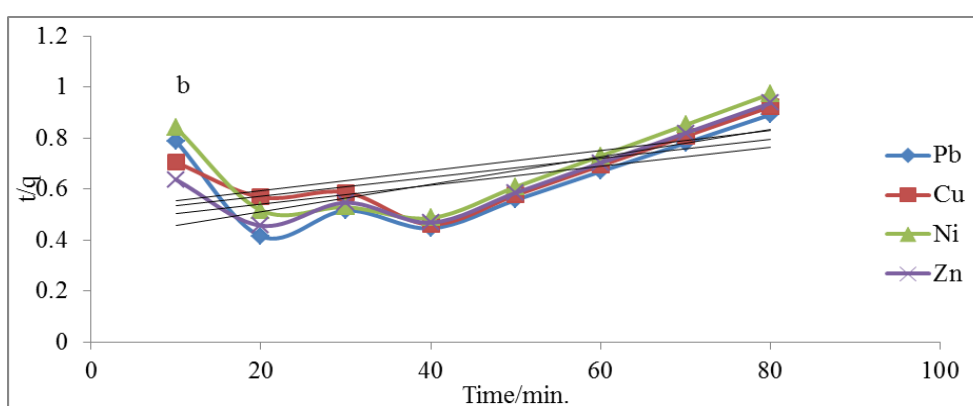


Fig. 4 (b) Pseudo-Second-order kinetics(plot of time vs. t/q) for heavy metal biosorption on PB.

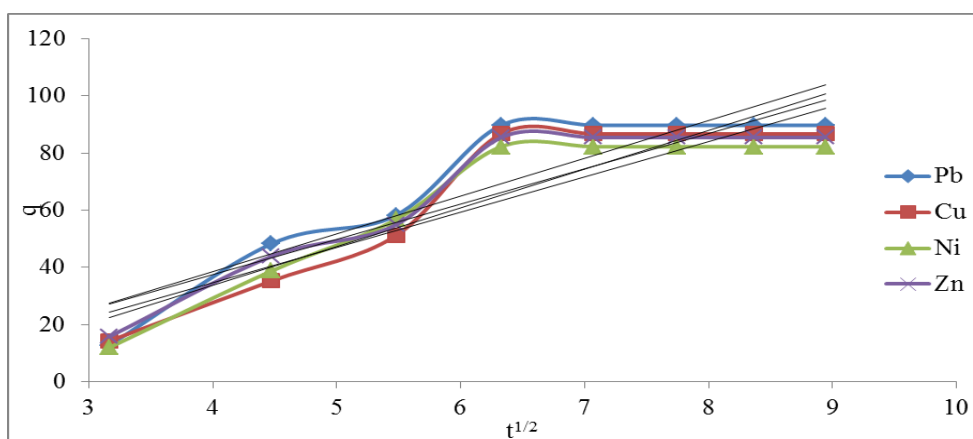


Fig. 4(c) Intraparticle model (plot of $t^{1/2}$ vs. q) for heavy metal biosorption on PB.

Table 4. Kinetic parameters for metal adsorption of Smart Pouch

Biomaterial (1.0/g)	Intraparticle diffusion parameters			Pseudo-second order constants		Pseudo-first order constants	
	R^2	C_i	k_{pi}	R^2	$k_{i(2)}(\text{L}/\text{min.})$	R^2	$k_{i(1)}(\text{L}/\text{min.})$
Pb	0.8275	14.20	13.21	0.2701	0.46	0.9986	2.07
Cu	0.8451	20.48	13.53	0.3851	0.49	0.9995	2.01
Ni	0.8332	14.80	12.34	0.2813	0.51	0.9991	2.07
Zn	0.8375	11.71	12.31	0.6057	0.28	0.9798	2.00

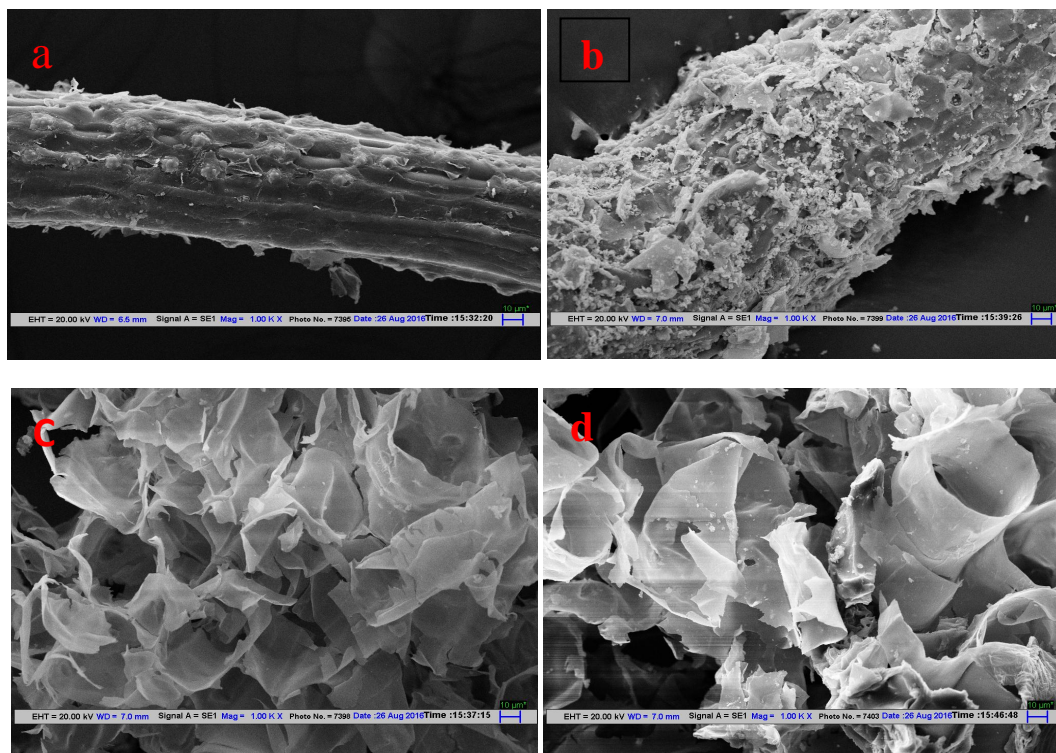
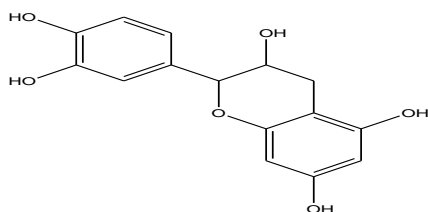


Fig. 5. SEM images of different orientation of biomaterial (a and c) before adsorption and (b and d) after adsorption.

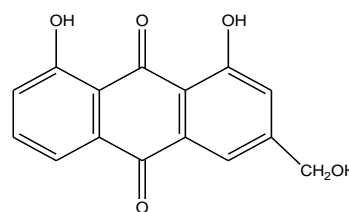
The SEM images of blended biomaterial at X1000 magnification prior to adsorption are shown in (Fig. 5a, and 5c) and afterward of surface assimilation of metals in (Fig. 5b, and 5d) observed at different orientations of the immiscible blend (coconut husk appears more in Fig. 5a, and 5c as well as *Aloe vera* leaf appears more in Fig. 5b, and 5d) using SEM analysis. There are noticeable changes to the surface morphology of the biomaterial as well as the creation of discrete aggregates on the biomaterial surface following metal removal via adsorption. Fig.5 showing that the biomaterial powder was an assemblage of fine particles (thread like structure due to coconut husk and like cavities due to *Aloe vera* leaf), but irregular. The particles were found to be of various dimensions consisting of steps and kinks on the external surface. Interaction of Pouch material with heavy metals has resulted in the formation of flake-like shiny deposition on its surface (Fig. 5b, d).

Catechin as the main constituent of coconut fibre or husk (Lima et al., 2015) possessing the structure placed herein Fig. 8 whereas the HOMO and LUMO orbitals are placed in Fig.6. However other extracts and fractions, also obtained from coconut husk and are rich in polyphenols, compounds such as catechins, epicatechins, tannins, and flavonoids etc. (Malik et al., 2017) but for computational chemistry, the main constituent i.e. catechin (Lima et al 2015) has been exploited for the present study. The Aloe leaves have multiple chemical constituents, out of which aloemodin ($C_{15}H_{10}O_5$) and aloetic acid ($C_{15}H_6N_4O_{13}$) are major components (Malik et al., 2017; Sharrif & Verma 2011) and catechin (Lima et al., 2015) as being rich in electron density are expected to offer the good adsorption centres for metals. HOMO and LUMO orbitals of catechin and aloemodin are obtained using Hyperchem 8.0 alongwith some other quantum parameters (Table 5).

Catechin (from coconut husk)



Aloe-emodin (from *Aloe vera*)



The quantum chemical parameters of major component of CH i.e. catechin and that of AV i.e. aloe-emodin, namely, the frontier molecular orbital energy reporting about E_{HOMO} and E_{LUMO} (energy of highest occupied molecular orbital and that of lowest unoccupied molecular orbital, respectively), the energy difference (ΔE) between E_{HOMO} and E_{LUMO} , and dipole moment (μ) are shown in Table 5 and Fig. 6. The quantum analysis predicts adsorption centers as identified with rich in electron density of the adsorbent molecules, hence, responsible for the interaction with heavy metal atom (Malik et al., 2017; Lima et al., 2015; Sharrif & Verma, 2011) The study provides the spatial distribution of

electronic density of the molecules and hence the chelating centers easily available on the blend. The structure of the components adsorbing the four studied metals is influenced by the electron density on the active centers of the biopolymer. The major component of Aloe vera (Aloe-emodin) (Sharrif & Verma, 2011) has greater electron density on oxygen present on the planar conjugated ring system of AV molecules. These atoms are expected to contribute to the interaction with the heavy metal. The outstanding adsorption on blend surface is due the low energy gap between the HOMO and LUMO energy levels of the molecules which also determines the extent of adsorption of the compound.

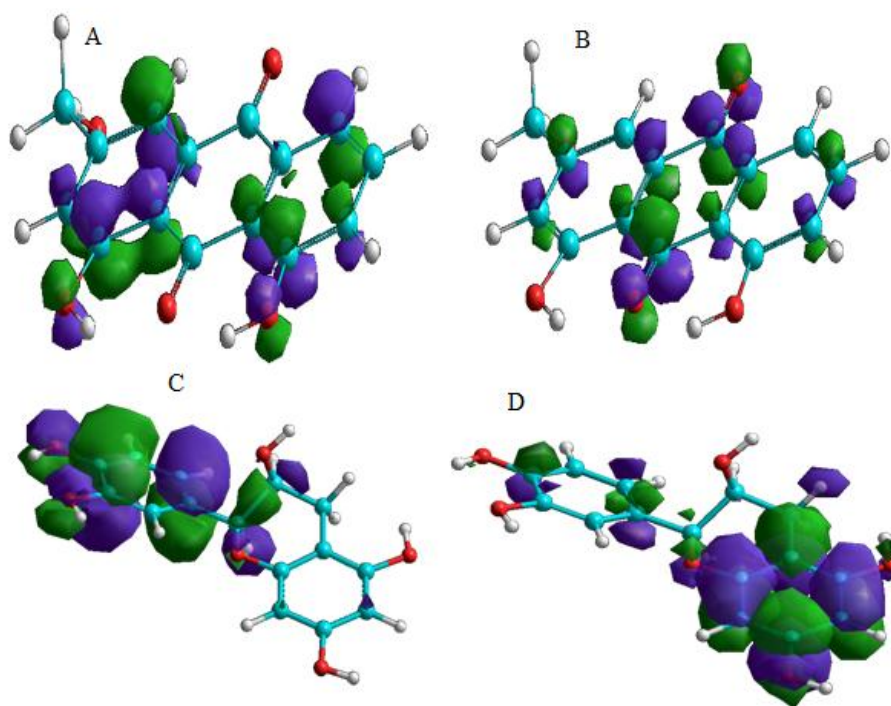


Fig. 6. HOMO and LUMO diagrams of AV (A and B) and CH (C and D) respectively

Table 5. Quantum chemical descriptors of CH (Lima et al,2015) and AV (Sharrif & Verma, 2011) (only major component)

Quantum descriptors	Coconut husk	Aloe vera
Total energy (kJ/mol)	-389392.91	-408736.59
Heat of formation (kJ/mol)	-871.12	-15881.82
E_{HOMO} (eV)	-8.81	-9.43
E_{LUMO} (eV)	-1.60	-1.60
Dipole moment(Debye)	3.06	1.68
Hydration energy(Kcal/mol)	-30.33Kcal/mol	-5.81 Kcal/mol
Polarizability	28.65 \AA^3	22.71 \AA^3
Surface area	365.4 \AA^2	489.49 \AA^2
Volume	777.88 \AA^3	649.65 \AA^3
Mass	290.27amu	260.16amu

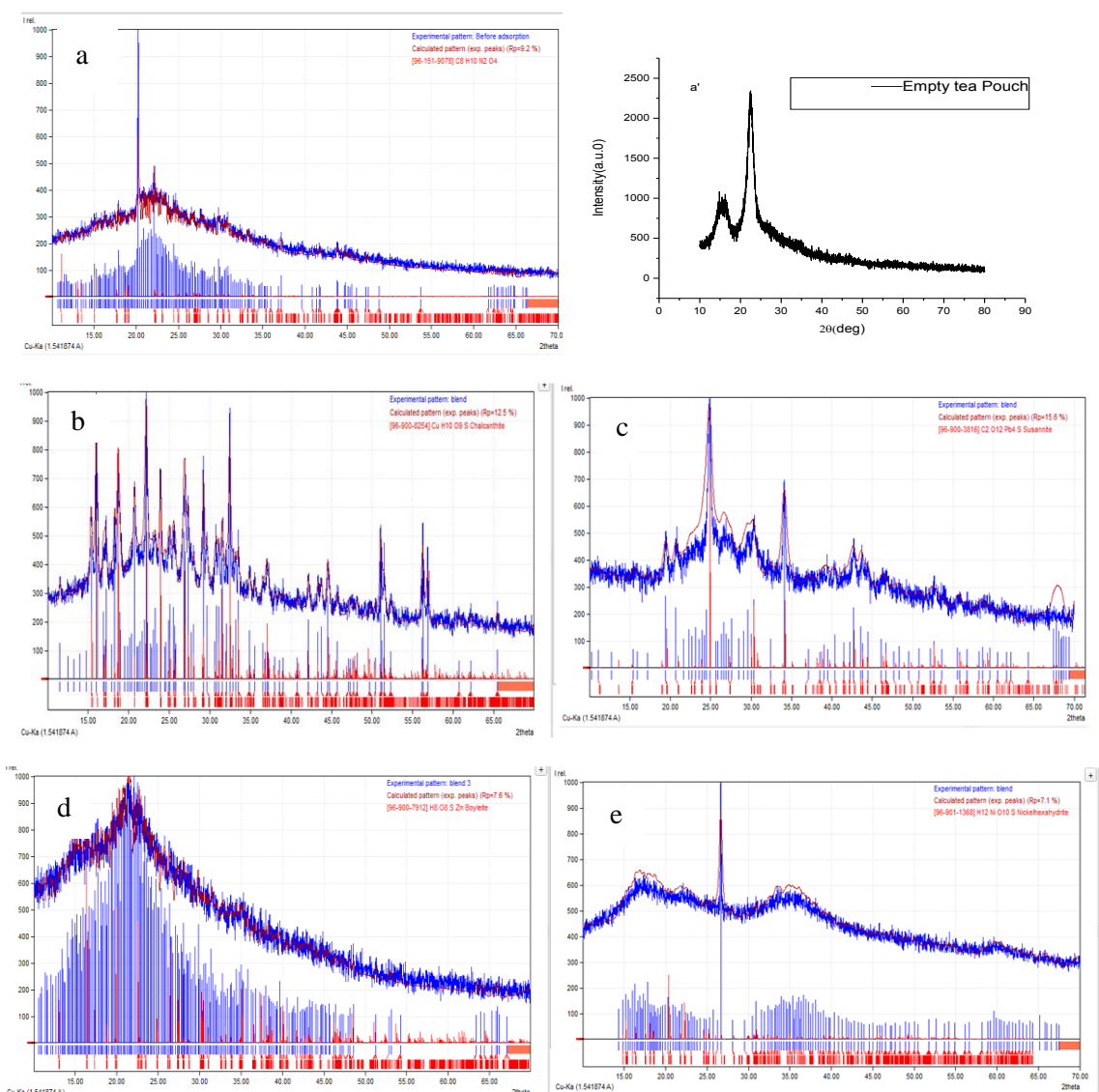


Fig. 7 (a) XRD peak positions of Biomaterial, (a') Empty tea Pouch before adsorption, and PB after adsorption of (b-Cu, c-Pb, d-Zn, e-Ni)

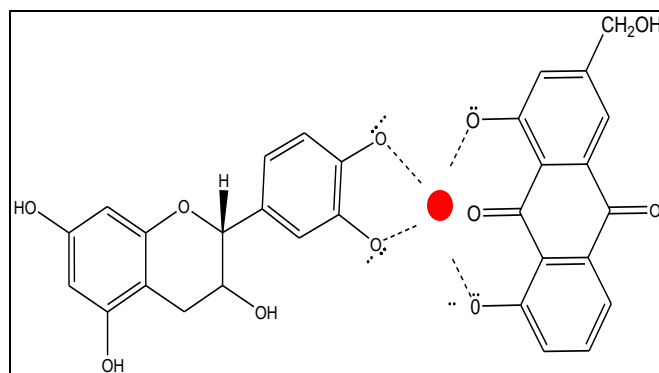


Fig. 8. Suggested mechanism of adsorption onto new biomaterial

Computational chemistry is an important and modern tool to access the required information about structure-activity relationship of different molecules and hence processes like heavy metal removal, corrosion (Pearson, 1988; Quraishi & Sharma, 2002; Sastri & Perumareddi 1997; Lukovits et al, 2001) etc. Based on the HOMO and LUMO structures of the major constituent of coconut husk (Lima et al, 2015) and *Aloe vera* i.e. Aloe-emodin (Sharrif & Verma, 2011), a theoretical approach for adsorption mechanism has been proposed in the present study. The molecules shown in (Fig.8) possess both anchoring groups i.e. $-OH$ and $-COC-$ acting as hard Lewis bases and π -electron cloud on benzene ring as soft base (HSAB principle). The computational study (Pearson, 1988) of the major component of CH as well as AV has facilitated the understanding about adsorption and it may be firmly believed that the effective binding may occur from 1,2 disubstituted side in comparison to 1,3 disubstituted side in case of catechin (Fig. 6) which is lucidly shown by HOMO and LUMO of catechin because the high electron density resides precisely at the HOMO of the flat aromatic ring. LUMO persists towards 1, 3 disubstituted side of the component with less available electron density and hence donation from this LUMO part becomes difficult. Moreover, the twisted nature of catechin (non-planar) facilitating binding of several metals simultaneously with lessened repulsions occurring among

the several metals. Aloe-emodin, on the other hand, being flat may show slightly lesser scope of binding with metals in comparison to catechin except Pouch ions (Table 6). It may also be noticed that the heavy metal may bind more effectively through the four oxygen atoms (one unit of each biopolymer with two O atoms due to newly developed and better interfacial interactions) as shown in Fig 8 or with two oxygen atoms of two similar constituents of CH and/or AV as well as with the other rich constituents of CH (Lima et al, 2015) and AV (Sharrif & Verma, 2011) possessing good donor groups like $-OH$, $-COC-$ etc. The contribution from these four oxygen atoms results into effective binding as compared to interactions offered by only two O atoms of a single unit of any biopolymer. All the three ions except Zn may show tendency towards partial complex formation with the hard base side of the coconut husk and *Aloe vera* i.e. $-OH$, $-COC-$ etc while for Zn being soft acid, electrostatic forces of attraction through π -electron density on aromatic rings of catechin and aloe-emodin may occur. Also, the high dipole moment, a measure of high electron density, which is 3.067 D for catechin and 1.68 D for Aloe-emodin given by quantum study (Table-5), hence, ready to donate electrons to the HM ions, as well as the E_{HOMO} and E_{LUMO} values confirm the ability of the biomaterial towards partial complex formation or electrostatic forces of attraction (Fig.6). Aloetic acid, another main constituent of *Aloe vera* has even higher side

dipole moment (5.692D) (Dahiya et al, 2016) may also show considerable contribution towards metal binding. Hence, the quantum study can be explored to understand the mechanism of adsorption by identifying the donation sites of the biosorbent.

The physiochemical properties of Cu, Pb, Ni and Zn divalent ions such as atomic weight, effective ionic radius, hydrated ionic radius and hydration energy, electronegativity etc (Lidec, 1998; Huheey et al., 1993; Dronskowski, 2005; Wieser & Coplen, 2009) placed in our earlier published article (Malik et al., 2017) have also been proved to be considerably responsible towards the nature and behavior of binding of metal ions onto PB surface. For example, chemical hardness essentially measures the resistance to change in the electron distribution in a collection of nuclei and electrons (Malik et al., 2017). Hydrated ionic radii of Pb is lowest but its diffusion coefficient at infinite dilution is highest along with its highest atomic weight and also the hydration energy etc. and therefore, the resultant of all such properties may undoubtedly become more suitable to the *Aloe vera* free active sites in two polymers' immiscible blend and similarly these behaviors for the other three metals may also be responsible partially or fully for the observed order of % removal using new Smart Pouch. When the hydration energy of both the constituents is considered (Table 5), CH possesses almost fivefold value than that of AV, and larger surface area of AV may facilitate the capture of larger Pb ions on sorption sites of Pouch containing AV as enclosed biomaterial. As there is difference between FTIR peaks (Fig.1), SEM images (Fig.5) and XRD pattern (Fig.7) before and after adsorption of HM ions in case of Pouch containing blend, it may be argued that there is increased attractive tendency for metals at the interface of CH and AV as well as at

their own surface due to van der Waal forces or any other electrostatic force of attraction. In addition to it, loosening of hydrogen bonds among the polymer units and/or layers may occur during blending process supplying more sites ready for adsorption, hence, the HM ions get trapped in between the two surfaces and/or layers. It is pertinent to mention that there is increased possibility of binding of HM ions due to the variety of active sites present on CH as well as AV individually and the newly generated sites available at the interface of the biosorbents due to blending and hence, synergizing performance of each other. Consequently, the uptake capacity of Pouch increases tremendously and almost complete removal for Pb and appreciable rise in % removal of other three metals also is observed in comparison to both the biopolymers when taken individually (Table 6). Such type of Smart Pouch filled with this biomaterial may be implemented at small industrial level for effective elimination of Pb, Cu, Ni and Zn metal ions. Hablot et al. also prepared renewable biocomposites by blending cellulose fibers with dimer fatty acid-based polyamides (DAPA) (Hablot et al, 2010; E et al, 2010) Despite of the immiscibility, the performance of cellulose was modified due to the strong interfacial interaction between the two components which also supports the present observations. Hence, batch experiments and physiochemical characteristics, in addition to the information provided by SEM, XRD and FTIR techniques and the computational study about available functional groups and active sites (Malik et al, 2015) present on the biosorbent, lucidly determine that the Smart Pouch as biosorbent has been proved an excellent tool for the effective removal of the four cations from aqueous medium because of its almost biodegradable nature ($\approx 90\%$) and remaining part of tea pouch can be composted.

Table 6. Maximum percentage elimination capacities (*Aloe vera*, Coconut husk and Smart Pouch with biomaterial) with each Biosorbent-1g, pH-6, Temperature-30°C, Agitation time-40 min, Agitation speed-200rpm

Metal	Maximum percentage removal (Aloe Vera)	Maximum percentage removal (Coconut Husk) (Malik et al., 2017)	Maximum percentage removal (New Pouch)
Pouch	90.21	72.40	99.99
Cu	81.50	88.61	93.21
Ni	76.91	80.90	91.97
Zn	85.12	67.63	86.41

CONCLUSION

Smart Pouch filled with *Aloe vera* and Coconut husk fine powders (synergistic behavior) can be used efficiently to manage the water contaminated with heavy metals (Pb, Cu, Ni and Zn) at different operating conditions through batch experiments. The order of accumulating tendency of the metals after optimization is Pb>Cu>Ni> Zn. The theoretical parameters obtained for the biomaterial using quantum chemical study also justify the findings. The adsorption isotherm constants i.e. Langmuir, Freundlich and Temkin very well favor the obtained order of removal. The characterization techniques (FTIR, SEM and XRD) also authenticate the results in understandable manner. The % removal of metals by PB was outstanding for Pb ions (almost 100%) whereas it was greater than 90% for Cu and Ni while for Zn>86%, proving that the Smart Pouch as recommendable substitute for a single biosorbent and may be implemented at small industrial level for efficient, convenient and low-cost elimination of Pb, Cu, Ni and Zn metals from waste water.

Acknowledgement

Authors are thankful to the University Grant Commission (UGC, New Delhi, India) with Ref. No-17-06/2012(1)EU-V for financial support to access this research work.

REFERENCES

Abdeen, Z., Mohammad, S. G. and Mohammad M. S. (2015). Adsorption of Mn (II) Ion on Polyvinyl Alcohol/Chitosan Dry Blending from aqueous

solution. Environ. Nanotechnol. Monit. Manag., 3(5);1-9.

Ali, A. S., Kazi I. W. and Ullah, N. (2015). New Chelating Ion-Exchange Resin Synthesized via the Cyclopolymerization Protocol and Its Uptake Performance for Metal Ion Removal, Ind. Eng. Chem. Res., 54; 9689–9698.

Arcana M. I., Bundjali B., Yudistira Y., Iyan. Jariah, B. and Sukria, L. (2007). Study on Properties of New Pouchs from Polypropylene with Polycaprolactone and Their Biodegradability. Polymer J., 39 (12);1337–1344.

Arief, V. O., Trilestari, K. Sunarso, J., Indraswati, N. Ismadji, S. (2008). Recent Progress on Biosorption of Heavy Metals from Liquids Using Low Cost Biosorbents: Characterization, Biosorption Parameters and Mechanism Studies, Clean, 36 (12);937 – 962.

Bueno, B. Y. M., Torem, M. L., Molina F. and de Mesquita L.M.S. (2008). Biosorption of lead(II), chromium(III) and copper(II) by *R. opacus*: Equilibrium and kinetic studies. Minerals Eng., 21;65–75.

Chiellini, E., Corti, A., Antone S. and Baci, R. (2006). Oxo-biodegradable carbon backbone polymers – oxidative degradation of polyethylene under accelerated test conditions. Polym. Degrad. Stabil., 91(11);2739–2747.

Dahiya, S. Lata, S. Kumar P. and Kumar, R. (2016). A descriptive study for corrosion control of low-alloy steel by *Aloe vera* extract in acidic medium, Corros Rev., 34; 241-248.

Das, S. K., Das A. R. and Guha, A. K. (2007). A study on the adsorption mechanism of mercury on *Aspergillus versicolor* biomass. Environ. Sci. Technol., 41;8281– 8287.

Dronskowski, R. (2005). Computational Chemistry of Solid State Materials. Weinheim, Germany: Wiley-vch Verlag GmbH & Co. KGaA.

Fiol, N., Villaescusa, I., Martínez, M., Miralles, N., Poch, J. and Serarols, J. (2006). Sorption of Pb(II), Ni(II), Cu(II) and Cd(II) from aqueous solution by olive stone waste. Sep. Purif. Technol., 50;132–140.

- Foo K. Y. and Hameed, B. H. (2010). Insights into the modeling of adsorption isotherm systems. *Chem Eng J.*, 156;2–10.
- Freundlich, H. M. F. (1906). *Über Die Adsorption in Lösungen*. *J. Phy. Chem.*, 57;385-370.
- Giusti, P., Lazzeri, L., Petris, S., Palla, M. and Cascone M.G. (1994). Collagen based new bioartificial polymeric materials. *Biomater.*, 15;1229–1233.
- Grimwood, B. E. and Ashman, F. (1975). Coconut palm products; their processing in developing countries.
- Hablot, E. Matadi, R. Ahzi and S. Averous, L. (2010a) Renewable biocomposites of dimer fatty acid-based polyamides with cellulose fibres: Thermal, physical and mechanical properties. *Compos. Sci. Technol.*, 70(3);504-509.
- Haghseresht F. and Lu, G. (1998). Adsorption characteristics of phenolic compounds onto coal-reject-derived adsorbents. *Energy Fuels.*, 12;1100–1107.
- Hameed, B. H. Tan I. A.W. and Ahmad, A.L. (2008). Adsorption isotherm, kinetic modeling and mechanism of 2,4,6-trichlorophenol on coconut husk-based activated carbon. *Chem Eng J.*, 144; 235–244.
- He, Z. L., Yang, X. E. and Stoffella, P. J. (2011). Trace elements in agro ecosystems and impacts on the environment. *J. Trace Elem. Med. Biol.*, 19;125–140.
- Ho, Y. S. Ng, J. C. Y. and McKay, G. (2000). Kinetics of pollutant sorption by biosorbents: review. *Sep and Puri Mets.*, 29(2);189–232.
- Huheey, E. Keiter E.A. and Keiter, R. L. (1993). *Inorganic Chemistry: Principles of Structure and Reactivity*, 4th edition. New York: HarperCollins College Publishers.
- Kaushal, A. and Singh, S. K. (2017). Removal of heavy metals by nanoadsorbents: A review. *J. environ. biotechnol. res.*, 6(1);96-104.
- Langmuir, I. (1916). *The Constitution and Fundamental Properties of Solids and Liquids*. Part I. Solids. *J. ACS.*, 38;2221-2295.
- Lide, D. R. (1998). *Handbook of Chemistry and Physics*, 79th ed.; CRC Press: Boca Raton, FL.
- Lukovits, E. Martín F. Ka and Zucchi. (2001). Corrosion inhibitors-correlation between electronic structure and efficiency. *Corrosion.*, 57;3–8.
- Malik, R., Dahiya S. and Lata, S., (2017). An experimental and quantum chemical study of removal of utmostly quantified heavy metals in wastewater using coconut husk: A novel approach to mechanism, *Int. J. Biol. Macromolec.*, 98;139–149.
- Malik, R. Lata, S. and Singhal, S. (2015). Removal Of Heavy Metal From Waste Water By The Use Of Modified Aloe Vera Leaf Powder, *Int. J. Basic & Appl. Chem. Sci.*, 5(2);6-17.
- Malik, R. Lata, S. Singhal, S. (2015) Evaluation of kinetics and adsorption isotherms for the Elimination of Pb (II) from aqueous solutions using Aloe barbadensis Miller Leaf Powder, *Pollution*, 1(4); 403-415.
- Matadi, R., Ahzi, S., Vaudemond, R., Ruch, D. and Averous, L. (2010b). Yield behaviour of renewable biocomposites of dimer fatty acid-based polyamides with cellulose fibres, *Compos Sci Technol.*, 70(3); 525-529.
- Miles, C. A. and Bailey, A. J. (2004). Studies of the collagen-like peptide (Pro-Pro- Gly). *J Mol Biol.*, 337;917–931.
- Okafor, P.C., Okon, P.U., Daniel, E.F. and Ebenso, E.E. (2012). Adsorption capacity of coconut (*Cocos nucifera* L.) shell for lead, copper, cadmium and arsenic from aqueous solutions. *Int. J. Electrochem. Sci.*, 7;12354-12369.
- Pagnanelli, F. Mainelli, S. Veglio F. and Toro, L. (2003). Heavy metal removal by olive pomace: Biosorbent characterization and equilibrium modeling, *J. Chem. Eng. Sci.*, 58; 4709 – 4717.
- Pearson, R.G. (1988). Absolute Electronegativity and Hardness: Application to Inorganic Chemistry, *Inorg. Chem.*, 27 (4);734–740.
- Pearson, R. G (2005). Chemical Hardness and Density Functional Theory, *J. Chem. Sci.*, 117(5);369–377.
- Pellera, F. M., Giannis, A., Kalderis, D., Anastasiadou K., Stegmann, R. and Wang, J. Y. (2012). Adsorption of Cu(II) Ions from Aqueous Solutions on Biochars Prepared from Agricultural By-Products. *J. Environ. Mngt.*, 96;35-42.
- Phuong, N. T. Guinault A. and Sollogoub, C. (2010). Miscibility and morphology of poly(lactic acid)/poly(b-hydroxybutyrate) blends. *Int. Conf. Adv. Mater Process Technol.*, AIP Conf Proc., 1315;173–178.
- Prasad M. and Saxena, S. (2004). Sorption mechanism of some divalent metal ions onto low-cost mineral adsorbent. *Ind Eng Chem Res.* 43 ;1512-1522.
- Quraishi M.A. and Sharma, H.K. (2002). 4-Amino-3-butyl-5-mercapto-1,2,4-triazole: a new corrosion

inhibitor for mild steel in sulphuric acid, *Mater Chem Phys.*, 78;18–21.

Rao M. and Bhole, A. G. (2001). Chromium removal by adsorption using fly ash and bagasse. *J. Indian Water Works Assoc.*, 33;97–100.

Reddy, N. and Yang, Y. (2005). Biofibers from agricultural byproducts for industrial applications. *Trends Biotechnol.*, 23 (1);22–27.

Romera, E. (2007). Comparative study of biosorption of heavy metals using different types of algae, *Bioresour Technol.*, 98; 3344 – 3353.

Sadeek, A., Negm, A.N., Hefnib H. H. H. and Wahab, M. M. A. (2015). Metal adsorption by agricultural biosorbents: Adsorption isotherm, kinetic and biosorbents chemical structures.

Int. J. Biol. Macromolec., 81;400–409.

Sastri V.S. and Perumareddi, J.R. (1997). Molecular orbital theoretical studies of some organic corrosion inhibitors. *Corrosion.*, 53;617–622.

Scott, G. (2000). 'Green' polymers. *Polym Degrad Stabil.*, 68(1);1–7.

Sharrif, M. M. and Verma, S .K (2011). Aloe vera, their chemicals composition and applications: a review. *Int. J. Biol. Med. Res.*, 2;466–471.

Shen, J. C. and Duvnjak, Z. (2004). Effects of temperature and pH on adsorption isotherms for

cupric and cadmium ions in their single and binary solutions using corncob particles as adsorbent, *Sep. Sci Technol.*, 39;3023 – 3041.

Slatter, D. A. Miles C. A. and Bailey, A. J. (2003). Asymmetry in the triple helix of collagen-like heterotrimers confirms that external bonds stabilize collagen structure. *J. Mol. Biol.*, 329;175–183.

Lima, E. B. C., Sousa, C. N. S., Meneses, L. N., Ximenes, N.C., Santos Júnior, M. A., Vasconcelos, G. S., Patrocínio, M. C. A., Macedo D. and Vasconcelos, S. M. M. (2015). Brazilian *Cocos nucifera* (L.) (Arecaceae): A phytochemical and pharmacological review. *Braz.J. Med and Bio Res.*, 48(11); 953–964.

Sun, X. F., Wang, S. G. Liu, X. W. Gong, Bao W. X., N. Gao and B.Y. Zhang, H.Y. (2008). Biosorption of Malachite Green from aqueous solutions onto aerobic granules: Kinetic and equilibrium studies. *Bioresour Technol.*, 99;3475-3483.

Wang, X. Sang, L. Luo D. and Li, X. (2011). From collagen–chitosan blends to three-dimensional scaffolds: the influences of chitosan on collagen nanofibrillar structure and mechanical property. *Colloids Surf B.*, 82; 233–240.

Wieser M.E. and Coplen, T.B. Atomic weights of the elements 2009. (IUPAC Technical Report), *Pure Appl. Chem.*, 83(2);359-396.

